Published in final edited form as:
Cell Host Microbe. 2009 October 22; 6(4): 331–342. doi:10.1016/j.chom.2009.09.004.

Mast Cells Augment Adaptive Immunity by Orchestrating Dendritic Cell Trafficking through Infected Tissues

Christopher P. Shelburne[1], **Hideki Nakano**[6], **Ashley L. St. John**[2], **Cheryl Chan**[1], **James B. McLachlan**[1], **Michael D. Gunn**[2,3], **Herman F. Staats**[1,2,3], and **Soman N. Abraham**[1,2,4,5]

[1] Department of Pathology, Duke University Medical Center, Durham, N.C. 27710, USA

[2] Department of Immunology, Duke University Medical Center, Durham, N.C. 27710, USA

[3] Department of Medicine, Duke University Medical Center, Durham, N.C. 27710, USA

[4] Department of Molecular Genetics & Microbiology, Duke University Medical Center, Durham, N.C. 27710, USA

[5] Program in Emerging Infectious Diseases, Duke-National University of Singapore Graduate Medical School, Singapore 169547

[6] Laboratory of Respiratory Biology, National Institutes of Environmental Health Sciences, National Institutes of Health, 111 T.W. Alexander Drive, Research Triangle Park, N.C. 27709, USA

Abstract

Mast cells (MCs) are best known for eliciting harmful reactions, mostly after primary immunity has been established. Here, we report that during *E. coli* infection, the primary humoral response in MC-deficient mice is significantly diminished, and was found to be less protective in a urinary tract infection (UTI) model compared to the response from MC-sufficient counterparts. MCs were found to recruit large numbers of dendritic cells (DCs) into the infected tissue site, which eventually migrated into draining lymph nodes (DLNs) over a prolonged time-course. This pattern of trafficking was facilitated by MC generated TNF, which increased the expression of E-selectin on local blood vessels. Antibody blockade of E-selectin inhibited DC recruitment into the site of infection and DLNs, and consequently impaired the primary humoral immune response. Thus, during infection, resident MCs contribute to the primary protective adaptive response through recruitment of DCs from the circulation into infected sites.

Introduction

MCs are well established as mediators in a variety of pathological conditions. For example, MCs are the principle effector cells responsible for the hives, eczema, hay fever and asthma associated with IgE mediated inflammatory reactions to further allergen exposure (Galli,

Correspondence and requests for materials should be addressed to: Christopher Shelburne, Ph.D., Department of Pathology, Duke University Medical Center, Durham, NC 27710, Phone: 919-684-3630, Fax: 919-684-2021, cps4@duke.edu.

CPS conducted most of the experiments and wrote most of the paper. HDG, HFS, HN, JBM, and SNA provided suggestions and discussion. ASJ and CC assisted with studies associated with DC trafficking to the lymph nodes. HFS, ASJ, and SNA helped with portions of the writing and editing of the manuscript.

Competing Interests Statement: The authors declare that they have no competing financial interests.

2000). However, in spite of the wealth of literature supporting their adverse effects, there is growing evidence that MCs contribute to the early and protective immune responses to microbial infection (Marshall, 2004). MCs are preferentially located at host–environment interfaces where they can encounter invading pathogens. Interactions with pathogens or pathogen products induce MCs to rapidly release a myriad of pre-stored and *de-novo* synthesized mediators (Gurish and Austen, 2001) that facilitate the recruitment of various immune cells to sites of infection or to distal nodes draining these sites. For instance, the rapid neutrophil response to different Gram positive and Gram negative bacterial infections has been linked to MC activation (Echtenacher et al., 1996; Malaviya et al., 1994; Mullaly and Kubes, 2006; Siebenhaar, 2007; Supajatura et al., 2001). Additionally, MC release of these mediators has been implicated in the enhanced influx and sequestration of T cells into distal DLNs following infection (McLachlan et al., 2003). The extravasation of circulating naïve T cells into DLN is triggered when MC-derived TNF percolates from the periphery into the nodes via lymphatic vessels (McLachlan et al., 2003). In spite of their potential to mobilize key immune cells during infection, a role for MCs in the development of the primary adaptive immune responses to pathogens has yet to be demonstrated.

Recently, several independent studies relating to vaccine development have reported reduced adaptive immune responses in MC-deficient mice after administration of various adjuvant compounds, including small MC-activating compounds (McLachlan et al., 2008), the TLR7 agonist imiquimod (Heib et al., 2007), or Complete Freund's Adjuvant (Gregory et al., 2005). Cumulatively, these observations point to a role for MCs in the development of primary adaptive immune responses. In some of these studies, MC activation was linked to enhanced migration of DCs from sites of vaccine delivery to the DLNs (Heib et al., 2007; McLachlan et al., 2008).

DCs are potent antigen presenting cells known to transport antigens from peripheral tissues to T-cell rich zones of secondary lymphoid tissue (Banchereau and Steinman, 1998). DC accumulation in DLNs is closely associated with a massive influx of naïve lymphocytes, a response that is functionally associated with optimal T-cell dependent immune responses (MartIn-Fontecha et al., 2003). It has also been shown that MCs promote the migration of epidermal Langerhans cells (LCs), a subset of DCs, following IgE mediated activation (Bryce et al., 2004; Jawdat et al., 2004). These studies raise the possibility that DCs may be mobilized by MCs to DLNs during microbial infection. Here, we examined the role of MCs in mobilizing DCs during bacterial infection employing multiple experimental models of *E.coli* infection and its resulting effect on the host's primary adaptive immune response.

Results

MCs contribute to the Primary Humoral Immune Response to Bacterial Infection

In light of the several lines of evidence pointing to a possible role for MCs in modulating primary adaptive immune responses to infection, we investigated the ability of a primary immune response evoked during challenge with uropathogenic *E.coli* strain, J96, by WT or MC-deficient mice to protect against a subsequent *E.coli* challenge. Since the innate immune system of MC-deficient mice is inherently compromised (Echtenacher et al., 1996; Malaviya, 1996), it was not possible to directly use MC-deficient mice for secondary challenge studies, as it would be difficult to distinguish between observations attributable to the innate or adaptive immune systems. Recently, Thumbikat et al demonstrated the protective capacity of *E. coli*–specific serum antibodies by infusing them into naïve mice and then showing that these passively immunized mice exhibited increased resistance to *E. coli*-induced bladder infections (Thumbikat et al., 2006). We attempted a similar experiment, to investigate the protective potential of the primary humeral immune response after *E. coli* challenge, developed in MC-sufficient or deficient hosts. For this experiment, we infused sera collected from MC-deficient

mice (Wsh) and WT mice, 14 days following footpad infection by *E. coli*, labeled with trinitrophenol (TNP) to serve as a unique antigen. We found that TNP-specific titers of antibodies in *E.coli*-infected WT mice were significantly higher than those observed in infected MC-deficient mice (Fig. 1A). These sera, as well as sera obtained from uninfected WT and MC-deficient mice, were then passively transferred to naive female mice by peritoneal injection before intravesicular challenge with 1×10^8 *E.coli* J96. As shown in Fig. 1B, bacterial numbers in the bladders of mice immunized with sera from WT mice were significantly reduced compared to controls, whereas this was not the case in mice immunized with sera from MC-deficient mice. Therefore, the antibody response evoked in MC-deficient mice is not only reduced, it is less protective than that of WT mice.

To verify the contribution of MCs to the development of primary humoral responses to *E.coli*, we compared the time course of the development of IgM and IgG antibodies in WT and MC-deficient mice following infection in a footpad model of infection. TNP-labeled *E. coli* were injected, as previously described, into the footpads of WT, MC-deficient (W/W^v), or control MC-deficient mice whose footpads had been repleted with WT MCs. After 7, 14 or 21 days, serum was collected and analyzed for TNP-specific IgM and IgG. Within 7 days, TNP-specific IgM had reached its maximal levels in WT mice, followed by a rapid decrease by 14 days (data not shown). Similarly, TNP-specific IgG was detected in WT mice by 7 days, but continued to increase until it reached maximal levels by 14 days (Fig. 1C). Comparatively, MC-deficient mice failed to induce high levels of TNP-specific IgM or IgG in the same time-course (data not shown and Fig. 1C, respectively). Reductions in total TNP-specific IgG in MC-deficient mice were reflected in all TNP-specific IgG isotypes relative to WT controls (data not shown) and repletion of MC-deficient footpads with MCs repaired the ability of these mice to generate TNP-specific antibody responses to levels seen in WT controls (Fig. 1C). These data suggest that the observed protective benefit of sera from MC-sufficient animals in the UTI challenge model may lie in the presence of increased, pathogen-specific antibody titers.

Since MC-derived TNF has been implicated in trafficking immune cells, we also investigated the specific contribution of this cytokine in the humoral immune response. We challenged $TNF^{-/-}$ or WT-MC footpad-repleted MC-deficient mice with TNP-labeled *E.* coli and compared their humoral responses. We found TNP-specific IgG in $TNF^{-/-}$ MC footpad-repleted MC-deficient mice was significantly less than deficient mice with WT-MC-repleted footpads (Fig. 1D). Collectively, these results reveal the vital role of MCs and MC-derived TNF in promoting primary humoral responses during bacterial infection.

MC-TNF Elicits Recruitment of DCs to Sites of *E. coli* Infection

Since it has been shown that MCs and MC-TNF promote the migration of epidermal LCs from the skin to DLNs following IgE mediated activation (Bryce et al., 2004; Jawdat et al., 2004), we hypothesized that one way MC-TNF may function to enhance adaptive immune responses during infection could be by inducing DC migration to DLNs. To investigate this possibility, we continued to use the footpad injection model for our primary challenge, injecting 1×10^5 *E. coli* J96 or saline control into the footpads of mice. After 3 hours, we examined cross-sections of mouse footpads for DC density and distribution by confocal microscopy. Surprisingly, we did not see a substantial change in the distribution of MHC Class II^+ LCs in the epidermal region of the footpad (Fig. 2A). However, compared to saline controls, we noticed a striking increase in MHC Class II^+ cells in the dermis around blood vessels (Fig. 2A). These cells were found to be positive for DC markers such as CD11c and CD11b, but not for the macrophage marker F4/80 (Supplemental Fig. 1). We confirmed that DCs were being recruited into the infection site using flow cytometry to analyze single cell suspensions of the footpad positive for the DC marker CD11c. By three hours after infection, we noted a significant recruitment

of DCs (2.3 fold over controls), which persisted for 12 hours before subsiding by 40 hours (Fig. 2B).

To confirm that MCs were active during DC recruitment after *E. coli* challenge, we stained tissue sections with Alexa-488-coupled avidin, which binds the MC granule component heparin. As shown in Fig. 2A, MCs are well represented in the dermis, proximal to blood-vessels in saline challenged tissues. However, in *E. coli* challenged footpad tissues MCs are less evident, suggesting that they have released their granule contents (Fig. 2A and Supplemental Fig. 1D). To demonstrate that MCs and MC-derived TNF are required for DC recruitment into inflamed tissue, we injected *E. coli* into footpads of MC-deficient mice or deficient animals whose footpads had been repleted with WT or $TNF^{-/-}$ MCs. As indicated in Fig. 2C, both MC-deficient mice and MC-deficient mice repleted with $TNF^{-/-}$ MCs failed to recruit DCs into the footpad by three hours, in contrast with MC-deficient mice repleted with WT MCs where significant recruitment occurred (Fig. 2C). These observations suggest that the recruitment of DCs observed at sites of *E. coli* infection is critically dependent on MC-TNF.

Since DCs are heterogeneous, with distinct subsets exhibiting differing functional capabilities, it was of interest to identify the principle DC subsets recruited into *E. coli*-infected tissue. Single cell suspensions were prepared from saline or *E. coli* challenged footpads, and assessed by flow cytometry employing antibodies against an assortment of DC surface markers (Table 1). This analysis allowed us to classify four DC subsets, designated FP-DC regions 1–4 (Table 1 and Fig. 2D)(Leon et al., 2007). Additional markers such as MHC Class II were also examined and are included in Supplemental Fig. 2. Comparison of the total numbers of each DC subset in the footpads 3 hours after challenge with either saline or *E. coli* revealed that a population of DCs that exhibits a phenotype of $CD11c^{mid}$ $CD11b^{+}$ $GR1^{-}$ (FP-R4) (Table 1,Fig. 2E), was substantially increased in response to *E. coli* challenge. A second subset of DCs which possessed a phenotype consistent with monocyte-derived DCs, $CD11c^{+}CD11b^{+}GR1^{+}$ (FP-R1) (Leon et al., 2007), also increased but only represented about 2% of the total FP-DC population (Table 1, Fig. 2E). Intriguingly, when we examined all 4 DC subsets for surface expression of the DLN homing chemokine receptor, CCR7, only the FP-R1 and FP-R4 subsets were significantly positive 12 hours after *E. coli* challenge (Supplemental Fig. 3). Taken together, these data reveal that MCs and MC-TNF recruit at least two DC subsets into the site of infection and these cells subsequently acquire the capability to traffic to the DLNs.

MC-TNF Induces E-selectin Expression on Vascular Endothelium and E-selectin Blockade Impairs DC accumulation in Infected tissues

Although MC-TNF appears to influence DC trafficking into the tissue, it is unclear, mechanistically, how this occurs. TNF is known induce the expression of adhesion molecules on blood vessel endothelium required for the recruitment of leukocytes into tissues (McHale et al., 1999). Therefore, we hypothesized that MC-TNF triggers the expression of adhesion molecules on blood vessel endothelium required for the recruitment of DCs into infected tissues. Confocal analysis of tissue sections derived from *E. coli* injected WT footpads revealed that several adhesion molecules, including E-selectin (CD62E), P-selectin (CD62P), ICAM-1, 2, and V-CAM were well expressed (data not shown). However, the most dramatic response 3 hours after *E. coli* challenge occurred with increases in E-selectin on blood vessel endothelium (Fig. 3A). Interestingly, this dramatic enhancement of E-selectin expression by 3 hours parallels the recruitment of DCs into the footpad (Fig. 2A and 2B). To determine if MC-TNF was required for the induction of E-selectin on footpad blood vessel endothelium, we challenged footpads of WT, MC-deficient, and MC-deficient mice repleted with WT or $TNF^{-/-}$ MCs with *E. coli* or saline. After three hours, footpads were collected, sectioned and stained for E-selectin and CD31 (a marker of blood vessel endothleium). Confocal microscopy

analysis revealed that *E. coli* challenge induced a 5.2-fold increase in the percentage of detectable blood vessel segments expressing E-selectin in WT tissue versus saline controls (Fig. 3B). Comparably, *E. coli* challenge of MC-deficient or $TNF^{-/-}$ MC-repleted MC-deficient footpads only induced a 2.5 or 2.6 fold induction of E-selectin expression on endothelial segments over saline controls, respectively (Fig. 3B). In contrast, challenge of WT-MC repleted MC-deficient footpads with *E. coli* resulted in a significant 4.25 fold increase in detectable E-selectin on endothelial segments that was comparable to WT controls (Fig. 3B). Thus, MC release of TNF induces optimal expression of E-selectin on blood vessel endothelium during infection.

To establish the relevance of MC-TNF induced increases of E-selectin on blood vessel endothelium to DC migration during infection, we examined DC migration within the context of E-selectin blockade. We hypothesized that infusion of antibodies against E-selectin would block the recruitment of DC subsets into the footpad. To assess this, we first injected mice with a monoclonal anti-E-selectin blocking antibody 2 hours prior to the injection of *E. coli* or saline in the footpad. Examination of footpad sections in mice injected with anti-E-selectin revealed that the antibody could be co-localized on footpad $CD31^{+}$ endothelium by 3 hours, and was detectable even at 24 hours (data not shown). We observed that E-selectin blockade profoundly interferes with *E. coli*-induced DC accumulation in the footpad (Fig. 3C). We also examined if E-selectin blockade was selective against particular DC subsets, however, we observed that it was uniformly effective against all recruited DC subsets (Fig. 3D). These results indicate that MC-TNF-induced E-selectin expression on vascular endothelium mediates the influx of DCs into infected tissue sites.

MC-TNF Promotes Accumulation of DCs in DLNs Following Infection

Since the primary immune response is dependent on the migration of antigen bearing DCs from infected sites to the DLNs, we examined the role for MCs and MC-TNF in the accumulation of DCs in the DLNs. Examination of single cell preparations of the popliteal DLNs at 12 hours after *E. coli* challenge demonstrated a significant (3-fold) increase in the total number of DCs (identified as $CD11c^{+}$ and MHC Class II^{+}) compared to saline controls (Fig. 4A). A maximal 7-fold increase in total DCs over saline controls was detected at 24 hours, followed by a substantial drop by 48 hours (2-fold increase over saline controls) (Fig. 4A). To determine if MCs contribute to DC accumulation in DLNs, we injected *E. coli* into the footpads of WT, W/W^{v}, or WT-MC footpad repleted MC-deficient mice. After 24 hours, single cell suspensions of DLNs were acquired and examined for total numbers of DCs. A significant deficiency in DC accumulation in the DLNs of MC-deficient mice was observed, compared to WT controls or to MC-deficient mice repleted with MCs (Fig. 4B). The reduced DC accumulation observed in MC-deficient mice was not due to a deficiency in tissue resident DCs (data not shown). It is also noteworthy that MC-dependent DC accumulation also correlated with optimal lymphocyte accumulation (McLachlan et al., 2003) (data not shown). Similar data was obtained in a UTI model, revealing that MCs are required for the optimal accumulation of DCs in the iliac DLNs after infection with *E. coli* in the bladder (Supplemental Fig. 4), thus illustrating that MCs influence DC migration in two separate models of *E. coli* infection.

To investigate the contribution of TNF to the mobilization of DCs into DLNs we compared DC numbers in DLNs of WT and $TNF^{-/-}$ mice following *E. coli* or saline challenge. A significant deficiency was observed in total DCs in the DLNs of $TNF^{-/-}$ animals, relative to WT controls (Fig. 4C). This mobilization defect was not due to an absence of footpad DCs or MCs in $TNF^{-/-}$ mice, as the numbers of both cell-types are comparable to those found in WT mice (data not shown). To determine if the TNF involved in DC accumulation was MC-derived, we compared DC numbers in MC-deficient mice that were repleted with MCs from WT or with $TNF^{-/-}$ mice. We found that, in contrast to MC deficient mice repleted with WT-MCs,

$TNF^{-/-}$ MC-repleted MC-deficient mice evoked markedly reduced levels of DC accumulation into DLNs (Fig. 4D). Therefore, as in the footpad, MC-derived TNF is required for the recruitment of DCs into DLNs.

While our data suggests that MC-TNF controls DC accumulation in DLNs through its influence on E-selectin expression on blood vessel endothelium at the site of infection, it is distinctly possible that MC-TNF might also influence DC trafficking to DLNs by acting on the distal DLN environment. Key chemokines known to influence this migratory pattern are CCL21 and CCL19, which are ligands for the surface receptor CCR7(Gunn et al., 1999). First, we examined the effects of anti-CCL21 or anti-CCL19 blockade on DC accumulation in DLNs after infection with *E. coli*. Anti-CCL21 blockade significantly interfered with DC and lymphocyte accumulation in DLNs compared to controls (Supplemental Fig. 5A), whereas anti-CCL19 blockade had no effect (Supplemental Fig. 5B). Therefore, we focused on the ability of MC-TNF to alter CCL21 levels during infection. To examine this, we first challenged WT footpads with *E. coli*, and then analyzed DLNs at various time points for the expression of CCL21 by ELISA. Injection of *E. coli* into footpads demonstrated that CCL21 levels are significantly increased in the DLNs by 3 hours, and remained elevated for up to twelve hours (Supplemental Fig. 5C). This increased CCL21 expression could be localized to cells present in the T-cell zones of DLNs of mice challenged with *E. coli*, but not in saline challenged mice (Supplemental Fig. 5D). To determine if MC-TNF is required for the induction of CCL21 in the DLN, we injected *E. coli* into the footpads of MC deficient mice and MC deficient mice repleted with $TNF^{-/-}$ MCs or WT MCs. Total protein was collected from DLNs after three hours and analyzed for the expression of CCL21. Although CCL21 was detectable in the DLNs of all of these mice, MC deficient and $TNF^{-/-}$ MC repleted MC deficient mice were unable to induce CCL21 to the higher levels observed in WT MC repleted W/W^{v} mice controls (Supplemental Fig. 5E). Collectively, these data suggest that MC-TNF has many targets that facilitate the enhanced migration of DCs, not only into the infected tissue site, but also into the DLNs.

Kinetics of DC Recruitment into Infected Tissues and Ensuing Migration to DLNs

Our data suggest that the majority of DCs reaching the DLNs from the infected sites are not originally tissue resident but recently recruited from the circulation. To clarify the nature of DC trafficking from the infected tissue to the DLN, we labeled all the cells in the footpad with the intravital dye CFSE (Legge and Braciale, 2003) and examined DC trafficking to the DLN after *E. coli* infection of the footpads. The instilled dose of CFSE was carefully titrated to ensure that all of the cells in the footpads were labeled without any excess CFSE label reaching the DLN. In this model, we expect that if most of the DCs that accumulate in the DLN during infection are derived from DCs resident to the footpad, then the majority of DCs should be labeled with CFSE. In contrast, if the majority of DCs are only transiently present in the tissue and recruited from the bloodstream into the tissue site in response to infection prior to their egress to the DLN, then we expect relatively few of the DCs in the DLN should be labeled with CFSE.

As shown in Fig. 5A, injection of 1×10^{-6} mmols of CFSE directly into the footpad fluorescently labels all of the cells present in the footpad, including the tissue resident DCs. After 4 hours, *E. coli* or saline was instilled into CFSE-labeled footpads and DLNs were acquired after 24 hours and analyzed for total $CFSE^{+}$ DC numbers. As demonstrated in Fig. 5B, 8.7% of the DCs that accumulate in the DLN after *E. coli* challenge are labeled with CFSE, indicating that the majority of the DCs in the DLN were not resident to the footpad at the time of bacterial challenge.

We undertook several controls to validate our experimental model and support the origin of our DC population as being non-tissue resident, yet having trafficked through the infected tissue. Importantly, non-DCs in the DLN remained unlabeled after 24 hours, establishing that

CFSE did not drain into the DLN and non-specifically label cells (Fig. 5B). CFSE-labeled DCs accumulated in T-cell zones of DLNs (data not shown) with a time-course commensurate with that observed in Fig. 5A, supporting the assumption that CFSE, itself, does not interfere with the ability of DCs to traffic in a normal manner (data not shown). Since there are two routes of entry for DCs into DLNs, through high endothelial venules (HEVs) or through the tissue draining lymphatics, it was also necessary to rule out the possibility that the majority of DCs within the DLN had trafficked into the DLN through the HEVs. Both plasmacytoid DCs (pDCs) and $CD8\alpha^+$ DCs are thought to enter the DLNs via the HEVs, and furthermore, pDCs may represent up to 70% of the total DC population in the DLNs of some mouse strains (Asselin-Paturel et al., 2001;Nakano et al., 2001). To clarify this, we examined DLN single cell suspensions from WT mice for pDCs ($CD11c^+/CD11b^{lo}/B220^+$) and $CD8\alpha^+$ DCs ($CD11c^+/CD11b^{lo}/B220^-/CD8\alpha^+$), which we found to collectively represent 10.9% and 15.6% of the total DC populations in saline and *E. coli* challenged mice, respectively (Supplemental Fig. 6). Most of the recruited DCs appeared in the $CD11c^+/CD11b^{hi}/GR1^-$ and $CD11c^+/CD11b^{mid}$ subsets (Supplemental Fig. 6). Additionally, extensive quantitative assessment of sections of DLNs 3, 6, 12, and 24 hours after challenge with *E. coli*, revealed that $CD11c^+$ and $CD11b^+$ cells traversing or in the lumen of HEVs are rare (<.5 $CD11c^+$ cells/HEV at 3, 6, 12, and 24 hours) (Supplemental Fig. 7). Taken together, these data validate our assumption that the relevant DC populations traffic through the site of infection and support the use of the CFSE labeling strategy to characterize the pattern of DC migration through infected footpad tissue.

To more effectively capture the DCs trafficking into the DLNs, which are presumably recently recruited DCs into infected sites, we labeled the footpad with CFSE 6 or 12 hours after challenge with *E. coli* or saline. By introducing the label significant periods after bacterial challenge, we expected to label recently recruited DCs in the footpad. We found that the accumulation of $CFSE^+$ DCs after 24 hours was 5% and 7%, respectively (Fig. 5C), a minority of the DC pool. This finding led us to hypothesize that the trafficking of recently recruited DCs to the DLNs was a gradual and continuous process rather than a single large bolus movement. To test this, we gave successive injections of CFSE at 0, 6 and 12 hours (multiple labels) after *E. coli* challenge to see if could induce a proportional increase in the number of $CFSE^+$ DCs accumulating in the DLN. As demonstrated in Fig. 5C, a significant three-fold increase in the total number of CFSE labeled DCs was seen in the DLN at 24 hours (27.2±13.7%) compared to saline challenge (8.6±4.2%). Cumulatively, our observations support the notion that following infection, DC recruitment into the infected site followed by egress into the DLN via the lymphatics occurs as a piece-meal and continuous process over an extended period of time.

Blockade of DC Recruitment into Infection Sites Impairs Development of Primary Adaptive Immune Responses

Taken together, our data suggest that during *E. coli* infection, MC-released TNF induces the expression of E-selectin on the endothelium of local blood vessels, allowing influx of bloodstream-derived DCs, and these recently recruited cells subsequently migrate to DLNs, initiating the development of a primary adaptive immune response. As such, we predicted that blockade of E-selectin expression at sites of infection should abrogate DC influx into these sites and ultimately into the DLNs and impair the development of the primary humoral response. We found that pretreatment with E-selectin-specific but not control rat IgG1 antibody significantly impaired the recruitment of total DCs into the DLNs following footpad challenge with TNP-labeled *E. coli* (Fig. 6A). Importantly, we were unable to detect the expression of E-selectin on the endothelium of the DLN at 3 (Fig. 6B), 6, 12, or 24 hours (data not shown) after infection with *E. coli*, confirming that E-selectin blockade of DC recruitment into the DLN was the result of its activity in the footpad. Additionally, administration of anti-E-selectin antibodies specifically blocked the development of TNP-specific humoral immune responses (Fig. 6C). Collectively, our data suggest that MCs modulate the primary adaptive immune

response during bacterial infections by inducing the recruitment of circulating DCs into sites of infection and subsequently into the DLNs.

Discussion

We have shown that during *E. coli* infection, tissue resident MCs play a critical role in drawing blood-borne DCs into infected sites, prior to their egress into secondary lymphoid organs, where they function to augment adaptive responses. In contrast to other models, which have shown a tissue resident origin of those antigen presenting cells mobilized by MCs in response to inflammatory stimuli (Bryce et al., 2004; Jawdat et al., 2004; Jawdat et al., 2006; Suto et al., 2006), we find that non-tissue-resident DCs derived from the bloodstream, primarily with a $CD11c^{mid}CD11b^{+}GR1^{-}$ phenotype, are recruited into infection sites prior to their egress to DLNs. In our infection model, we observed that the trafficking of DCs through infected tissues and into the DLN does not involve bulk flow, but occurs in an incremental and continuous manner. This could reflect the previously reported piece meal activation response of MCs to infecting *E. coli* (Malaviya R, 1994) and the ensuing MC-initiated changes to the vascular endothelium, such as the observed up-regulation of E-selectin and culminating in the continual recruitment of new DCs into infected tissues. In spite of the continual flow of DCs into DLNs, it is noteworthy that maximal DC movement was achieved by 24 hours, which coincides with the previously reported time frame for maximal sequestration of circulating lymphocytes in the DLN following *E. coli* infection, a trafficking response also mediated by peripheral MCs (McLachlan et al., 2003). Therefore, during *E. coli* infections, tissue resident MCs appear to regulate the coordinate mobilization into the DLNs of both DCs and T cells, the two cell types principally involved in the induction of primary immune responses. Coincident mobilization of antigen presenting DCs and T cells into DLNs should greatly enhance the probability of interaction between antigen presenting DCs and naïve antigen-specific T cells. The functional relevance of MC mediated immune cell trafficking into DLNs is illustrated by the finding that, compared to WT mice, titers and protective abilities of humoral antibodies produced in MC-deficient mice are significantly diminished (Fig. 1). These results and our interpretation could explain why, after primary challenge, we observed that sera derived from WT mice offered significantly more protection than sera from MC-deficient mice when recipient mice were challenged in the urinary tract with *E. coli* (Fig. 1). Potentially, MCs can enhance protective adaptive immune responses not only *to E. coli* in the footpad and UTI models of infection, but in many body sites and, likely, in response to a range of pathogens.

MCs are located not only at host-environment interfaces but, additionally, many MCs are found lining the host vasculature (Marshall and Jawdat, 2004). TNF, which is typically pre-stored within MC granules and released immediately after MC activation, is well known for promoting vascular permeability (Bradley, 2008). Previously, TNF from peripheral MCs was identified as the primary MC determinant responsible for mediating increased sequestration of lymphocyctes in DLNs following infection, likely acting, at least in part, through the up-regulation of the vascular cell adhesion molecule-1 (VCAM-1) on high endothelial venules (McLachlan et al., 2003). Here, we demonstrated that the influx of specific subsets of circulating DCs into sites of infection was mediated by MC-TNF through its action both at the site of infection and in the distal DLNs. We see MC-TNF induces both up-regulation of E-selectin expression on endothelial cells in neighboring blood vessels in the site of infection, as well as enhanced CCL21 production in the DLN. The contribution of E-selectin to the entry of DCs into infection sites and the contribution these cells play to the developing immune response was evident from the finding that a monoclonal antibody directed at E-selectin could not only block the influx of DC subsets into sites of infection but also significantly reduced the primary immune response to infection. MC-TNF was also found to enhance expression of the CCL21 chemokine in the DLN after *E. coli* challenge. Presumably, MC-TNF acts by flowing into the DLN and activating $TNFR^{+}$ stromal or endothelial cells to increase their

expression of CCL21. This remote control mechanism, first suggested for the MCP-1 chemokine (Palframan et al., 2001), may be a major mechanism by which the inflammatory state of the peripheral tissue is communicated to the DLN environment. Collectively, these data emphasize the combinatorial function of MC-TNF targets to optimize DC trafficking through infected sites and to the DLN.

Finally, in contrast to other models of inflammation that indicate that MCs have a limited role in the development of primary immune responses, or that they have primarily a pathological role (Galli et al., 2005), our data suggests that MCs play a key role in the development of primary immune responses to infection. Although the adaptive immune response evoked here in our studies are largely cleared by the innate immune response before the humoral response is detectable, this response will likely confer protection to the host during subsequent *E. coli* infections, and may be particularly important in the UTI model, where a reservoir of persistent bacteria can remain after innate clearance (Mysorekar and Hultgren, 2006). Nevertheless, these results expand our view of tissue resident MCs by extending their known sphere of influence. MCs appear not only to act locally within the site of infection through innate recognition of pathogens but, additionally, they amplify adaptive immunity indirectly, through the recruitment of DCs. In this way, MCs function both in the local site of infection and the distal DLN to promote pathogen control and, similarly, act with a broad temporal scope, being one of the first cells to respond to invading pathogens yet greatly influencing the long term immunological memory to pathogens. This recognition could potentially be harnessed for immuno-prophylactic or therapeutic purposes against harmful infectious diseases.

Methods and Materials

Mice and MC Reconstitutions

Male MC-deficient WBB6F1-W/W^{v} mice, congenic littermate control WWB6F1-+/+ mice, MC-deficient W^{sh}/W^{sh}, TNF$^{-/-}$ (B6;129S6-*Tnf*^{tm1Gk1}) mice and B6129SF2/J controls were from Jackson Laboratories. TNF$^{-/-}$ mice on a C57BL/6 background were purchased from B&K Universal. C57BL/6 mice were obtained from the NCI production facility. Mice were housed in the Duke University Vivarium until experiments were performed. For reconstitutions, MCs were prepared and transferred into the footpads of recipient mice as described in Supplemental Methods. All experimental protocols were approved by the Duke University Institutional Animal Care and Use Committee.

Reagents

Labeled and unlabeled antibodies against MHC Class II (Clone M5/114.15.2), CD8α (Clone 53-6.7), CD11b (Clone M1/70), CD11c (Clone HL3), CD19 (Clone 1D3), CD40 (Clone HM40-3), CD86 (Clone GL1), B220 (Clone RA3-6B2), GR1 (Clone RB6–8C5), F4/80 (Clone BM8) and CCR7 (Clone EBI-1) were from e-Biosciences or BD Biosciences. Polyclonal anti-Kit, anti-CCL21 and anti-CCL19 were from R&D Systems. Anti-CD62E (clone 9A9) was a kind gift of Klaus Ley (University of Virginia, Charlottesville, VA). 2,4-carboxy-fluorescein di-succimidyl-ester (CFSE) and Alexa-488 labeled avidin are from Molecular Probes. All secondary isotype matched controls are from BD Biosciences. All polyclonal controls are from Jackson ImmunoResearch.

Footpad Infection Model

For humoral or DLN studies, 1×10^{6} TNP-labeled *E. coli* strain J96 or 1×10^{5} unlabeled *E. coli* strain J96 was subcutaneously injected into footpads in a 20ul volume, respectively. *E. coli* was labeled with TNP as described in Supplemental Methods. For anti-CD62E blocking studies, 100μg of the 9A9 monoclonal was injected into the tail-vein 2 hours prior to *E. coli* or saline challenge.

Urinary Tract Infection Model

UTIs in mice were established by instilling 1×10^8 J96 *E. coli* in a 30μl volume into the bladder through a catheter inserted into the ureter of anesthetized female mice. For protection studies, 150μl serum from *E. coli* immunized mice was intraperitoneally injected into recipient WT female mice, 24 hours prior to bladder challenge with J96 *E. coli*. After 24 hours, bladders were collected from sacrificed mice and homogenized in .5% Triton-X in PBS with 3 pulses of a Fastprep 120 rotary tissue homogenizer (Thermo). Samples were diluted and plated onto MacKonkey agar plates. Total colony forming units of *E. coli* were evaluated by counting.

Immunofluorescence and confocal analysis

Prepared DLN or footpad sections were stained with labeled primary antibodies as indicated. For CD11c staining, sections were labeled with anti-CD11c (Clone HL3), followed by detection with biotinylated anti-hamster and strepavidin-APC. Confocal images were obtained with a 3-Laser Nikon Confocal Laser Scanning Instrument (Nikon Instruments). Images were obtained using EZ-C1 Nikon software (Silver Version 2.01). Threshold values were determined using the appropriate isotype-matched controls. A channel series approach was used to ensure no spectral overlap between fluorescent signals.

Isolation and Flow Cytometric Analysis of Single Cell Suspensions of footpads or DLNs

At the indicated times, footpads or DLNs were isolated and minced, followed by incubation in 100U/ml Collagenase A (Sigma) for 30 minutes at 37°C. Samples were then pressed through a 70μM cell straining filter (BD Biosciences) and washed. Samples were then incubated with the indicated antibodies to detect DCs or DC subsets and analyzed using a FACscalibur or LSRII flow cytometer (BD Biosciences). For complete methods see the Supplemental Methods section.

DC Tracking Studies

1×10^{-6} mmols of CFSE or vehicle was instilled into footpads in a 20 μl volume. *E. coli* or saline was instilled after 4 hours. For post *E. coli* challenge labeling studies, CFSE was instilled at $.75\times10^{-6}$ mmols in 20μl at the indicated times after saline or *E. coli* challenge. After 24 hours, single cell suspensions of DLNs were stained as indicated and analyzed by flow cytometry.

ELISAs

Blood was collected via the tail vein at days 7, 14, and 21 post-challenge. Antigen specific titers of anti-TNP IgM, IgG, or IgG isotypes were determined by capture ELISA using TNP-OVA (Alexis), and anti-IgM, IgG, or IgG isotypes (Southern Biotech). The data presented is the reciprocal $\log_2$ dilution of the last sample OD that was 2 fold higher than the naïve sample OD. The geometric mean titer and standard deviation were calculated using the $\log_2$ endpoint titers. Statistics were first performed on the $\log_2$ titers prior to conversion.

Statistical Analysis

Data was analyzed for statistical significance as indicated with one-way ANOVA and Tukey's post-test with Graphpad Prism, or unpaired Student's *t*-test with Microsoft Excel. Differences between groups were considered significant at $p\leq0.05$.

Supplementary Material

Refer to Web version on PubMed Central for supplementary material.

Acknowledgments

This work was supported by funds from the National Institutes of Health RO1-DK077159, R37-DK050814, R21-DK077307 and R01-AI 50021, the Sandler Foundation for Asthma Research and the Duke University's CTSA grant UL1RR024128 from NCRR/NIH.

References

Asselin-Paturel C, Boonstra A, Dalod M, Durand I, Yessaad N, Dezutter-Dambuyant C, Vicari A, O'Garra A, Biron C, Briere F, Trinchieri G. Mouse type I IFN-producing cells are immature APCs with plasmacytoid morphology. Nat Immunol 2001;2:1144–1150. [PubMed: 11713464]

Banchereau J, Steinman RM. Dendritic cells and the control of immunity. Nature 1998;392:245–252. [PubMed: 9521319]

Bradley JR. TNF-mediated inflammatory disease. J Pathol 2008;214:149–160. [PubMed: 18161752]

Bryce PJ, Miller ML, Miyajima I, Tsai M, Galli SJ, Oettgen HC. Immune sensitization in the skin is enhanced by antigen-independent effects of IgE. Immunity 2004;20:381–392. [PubMed: 15084268]

Echtenacher B, Mannel DN, Hultner L. Critical protective role of mast cells in a model of acute septic peritonitis. Nature 1996;381:75–77. [PubMed: 8609992]

Galli SJ. Allergy. Curr Biol 2000;10:R93–95. [PubMed: 10679332]

Galli SJ, Nakae S, Tsai M. Mast cells in the development of adaptive immune responses. Nat Immunol 2005;6:135–142. [PubMed: 15662442]

Gregory GD, Robbie-Ryan M, Secor VH, Sabatino JJ Jr, Brown MA. Mast cells are required for optimal autoreactive T cell responses in a murine model of multiple sclerosis. Eur J Immunol 2005;35:3478–3486. [PubMed: 16285014]

Gunn MD, Kyuwa S, Tam C, Kakiuchi T, Matsuzawa A, Williams LT, Nakano H. Mice lacking expression of secondary lymphoid organ chemokine have defects in lymphocyte homing and dendritic cell localization. J Exp Med 1999;189:451–460. [PubMed: 9927507]

Gurish MF, Austen KF. The diverse roles of mast cells. J Exp Med 2001;194:F1–5. [PubMed: 11435478]

Heib V, Becker M, Warger T, Rechtsteiner G, Tertilt C, Klein M, Bopp T, Taube C, Schild H, Schmitt E, Stassen M. Mast cells are crucial for early inflammation, migration of Langerhans cells, and CTL responses following topical application of TLR7 ligand in mice. Blood 2007;110:946–953. [PubMed: 17446350]

Jawdat DM, Albert EJ, Rowden G, Haidl ID, Marshall JS. IgE-mediated mast cell activation induces Langerhans cell migration in vivo. J Immunol 2004;173:5275–5282. [PubMed: 15470073]

Jawdat DM, Rowden G, Marshall JS. Mast cells have a pivotal role in TNF-independent lymph node hypertrophy and the mobilization of Langerhans cells in response to bacterial peptidoglycan. J Immunol 2006;177:1755–1762. [PubMed: 16849485]

Legge KL, Braciale TJ. Accelerated migration of respiratory dendritic cells to the regional lymph nodes is limited to the early phase of pulmonary infection. Immunity 2003;18:265–277. [PubMed: 12594953]

Leon B, Lopez-Bravo M, Ardavin C. Monocyte-derived dendritic cells formed at the infection site control the induction of protective T helper 1 responses against Leishmania. Immunity 2007;26:519–531. [PubMed: 17412618]

Malaviya R, Ikeda T, Ross E, Abraham SN. Mast cell modulation of neutrophil influx and bacterial clearance at sites of infection through TNF-alpha. Nature 1996;381:77–80. [PubMed: 8609993]

Malaviya RRE, Jakschik BA, Abraham SN. Mast cell degranulation induced by type 1 fimbriated Escherichia coli in mice. Journal of Clinical Investigation 1994;93:1645–1653. [PubMed: 7512987]

Malaviya R, Ross E, Jakschik BA, Abraham SN. Mast cell degranulation induced by type 1 fimbriated Escherichia coli in mice. J Clin Invest 1994;93:1645–1653. [PubMed: 7512987]

Marshall JS. Mast-cell responses to pathogens. Nat Rev Immunol 2004;4:787–799. [PubMed: 15459670]

Marshall JS, Jawdat DM. Mast cells in innate immunity. J Allergy Clin Immunol 2004;114:21–27. [PubMed: 15241339]

MartIn-Fontecha A, Sebastiani S, Hopken UE, Uguccioni M, Lipp M, Lanzavecchia A, Sallusto F. Regulation of dendritic cell migration to the draining lymph node: impact on T lymphocyte traffic and priming. J Exp Med 2003;198:615–621. [PubMed: 12925677]

McHale JF, Harari OA, Marshall D, Haskard DO. Vascular endothelial cell expression of ICAM-1 and VCAM-1 at the onset of eliciting contact hypersensitivity in mice: evidence for a dominant role of TNF-alpha. J Immunol 1999;162:1648–1655. [PubMed: 9973425]

McLachlan JB, Hart JP, Pizzo SV, Shelburne CP, Staats HF, Gunn MD, Abraham SN. Mast cell-derived tumor necrosis factor induces hypertrophy of draining lymph nodes during infection. Nat Immunol 2003;4:1199–1205. [PubMed: 14595438]

McLachlan JB, Shelburne CP, Hart JP, Pizzo SV, Goyal R, Brooking-Dixon R, Staats HF, Abraham SN. Mast cell activators: a new class of highly effective vaccine adjuvants. Nat Med 2008;14:536–541. [PubMed: 18425129]

Mullaly SC, Kubes P. The role of TLR2 in vivo following challenge with Staphylococcus aureus and prototypic ligands. J Immunol 2006;177:8154–8163. [PubMed: 17114491]

Mysorekar IU, Hultgren SJ. Mechanisms of uropathogenic Escherichia coli persistence and eradication from the urinary tract. Proc Natl Acad Sci U S A 2006;103:14170–14175. [PubMed: 16968784]

Nakano H, Yanagita M, Gunn MD. CD11c(+)B220(+)Gr-1(+) cells in mouse lymph nodes and spleen display characteristics of plasmacytoid dendritic cells. J Exp Med 2001;194:1171–1178. [PubMed: 11602645]

Palframan RT, Jung S, Cheng G, Weninger W, Luo Y, Dorf M, Littman DR, Rollins BJ, Zweerink H, Rot A, von Andrian UH. Inflammatory chemokine transport and presentation in HEV: a remote control mechanism for monocyte recruitment to lymph nodes in inflamed tissues. J Exp Med 2001;194:1361–1373. [PubMed: 11696600]

Siebenhaar F, Syska W, Weller K, Magerl M, Zuberbier T, Metz M, Maurer M. Control of Pseudomonas aeruginosa skin infections in mice is mast cell-dependent. Am J Pathol 2007:1910–1916. [PubMed: 17525259]

Supajatura V, Ushio H, Nakao A, Okumura K, Ra C, Ogawa H. Protective roles of mast cells against enterobacterial infection are mediated by Toll-like receptor 4. J Immunol 2001;167:2250–2256. [PubMed: 11490012]

Suto H, Nakae S, Kakurai M, Sedgwick JD, Tsai M, Galli SJ. Mast cell-associated TNF promotes dendritic cell migration. J Immunol 2006;176:4102–4112. [PubMed: 16547246]

Thumbikat P, Waltenbaugh C, Schaeffer AJ, Klumpp DJ. Antigen-specific responses accelerate bacterial clearance in the bladder. J Immunol 2006;176:3080–3086. [PubMed: 16493067]

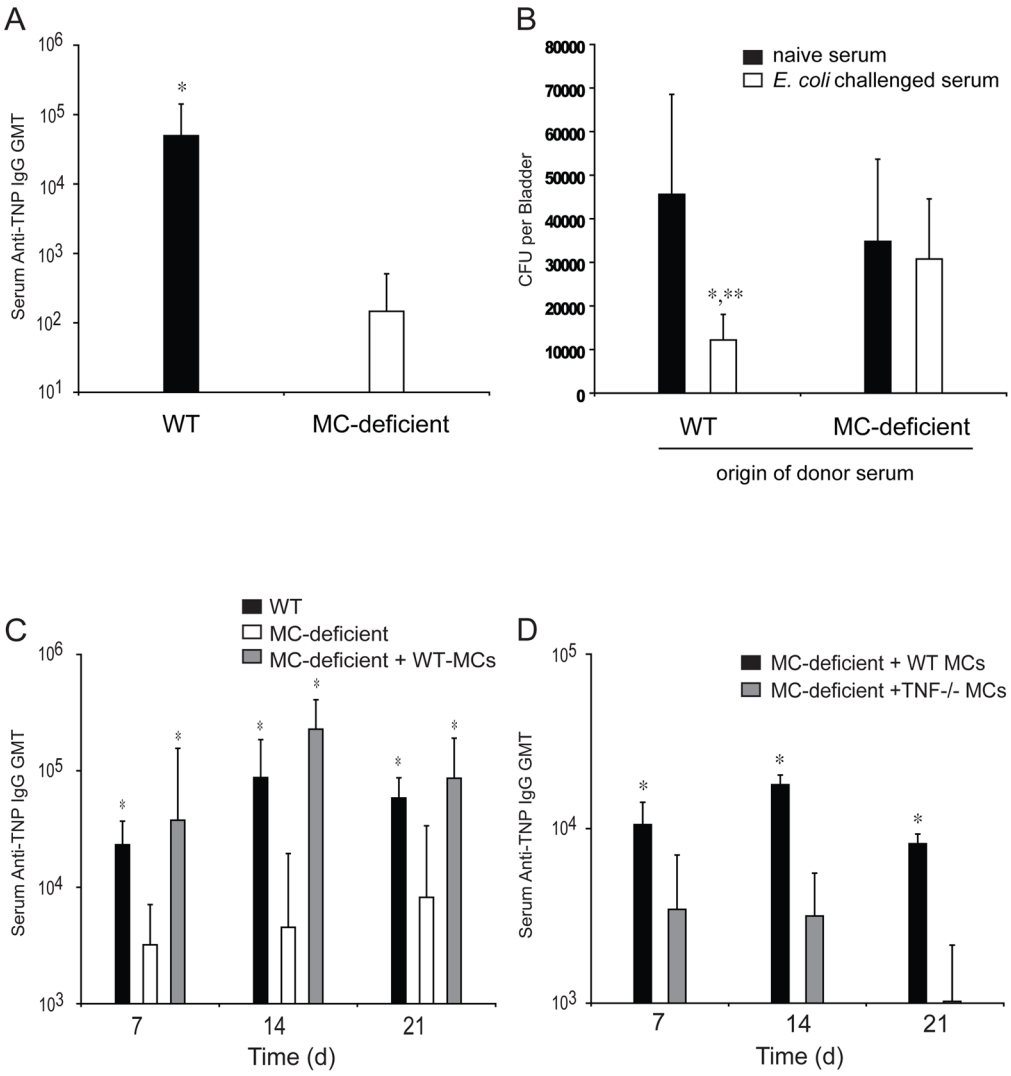

Figure 1. MCs are Required for the Maximal Induction of a Protective Primary Humoral response to *E. coli*

(A) GMT of TNP-specific serum IgG in WT and MC-deficient W^{sh}/W^{sh} (Wsh) mice 14 days after injection with $1X10^6$ TNP-labeled *E. coli*. N=9–11. $^*p<0.05$ compared to Wsh mice using unpaired Student's t-test. (B) The number of *E. coli* colony forming units (CFU) per bladder of WT mice that received 150μl serum from naïve or TNP-*E. coli* immunized WT or Wsh mice. N=9–11. $^*p<0.05$ comparing responses in recipient mice that received serum from naïve or *E. coli* challenged mice, and $^{**}p<0.05$ comparing the responses between recipient mice that received serum from *E. coli* challenged WT and Wsh mice. (C) GMT of TNP-specific serum IgG in WT, MC-deficient W/W^v, and footpad WT-MC-repleted W/W^v mice injected with $1X10^6$ TNP-labeled *E. coli*. N=12 for WT, N=14 for W/W^v, and N=5 for WT-MC reconstituted W/W^v samples. $^*p=0.001$ compared to W/W^v mice. (D) GMT of TNP-specific serum IgG in footpad WT-MC-repleted or $TNF^{-/-}$ MC-repleted W/W^v mice injected with $1X10^6$ TNP-labeled *E. coli*. n=5 for each group. $^*p=0.001$. Data in B–D was analyzed for statistical significance with one-way ANOVA and Tukey's post-test. Graphical bars represent the mean ±S.D.

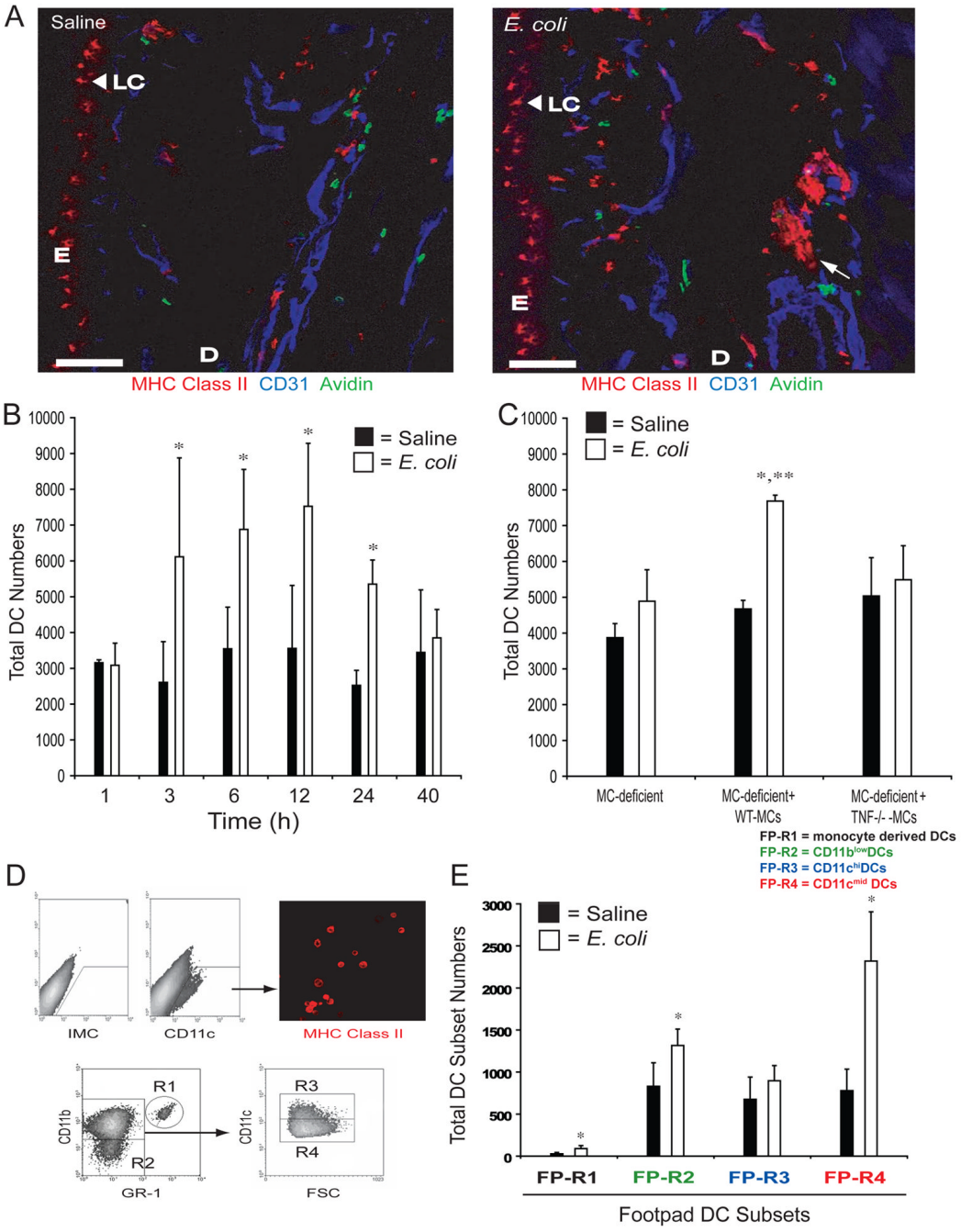

Figure 2. Challenge of Footpads with *E. coli* induces a MC-TNF Dependent Increase in DC Numbers

(A) Analysis of WT footpad, 3 hours after injection of *E. coli* or saline, for MHC Class II (DCs), CD31 (blood vessel endothelium), and avidin (MCs) by confocal microscopy. Scale bars = 100μM. E = epidermis, D = Dermis, LC = Langerhans cells (arrowheads). The arrow denotes a DC bundle. (B) Total number of $CD11c^+$ DCs in single cell suspensions of footpads at the indicated time-points. N=4–5 for each time-point. $^*p<0.05$ compared to saline controls. Data was analyzed for statistical significance with one-way ANOVA and Tukey's post-test. (C) Total number of $CD11c^+$ DCs in single cell suspensions of W/W^v, WT-MC or $TNF^{-/-}$ MC repleted W/W^v footpads, 3 hours after saline or *E. coli* challenge. N=4 for each sample. $^*p<0.05$

compared to saline controls and $^{**}p<0.05$ comparing *E. coli* challenged WT-MC repleted W/W^v footpad samples to W/W^v and TNF$^{-/-}$ MC-repleted W/W^v samples. Data was analyzed for statistical significance with one-way ANOVA and Tukey's post-test. (D) The gating strategy to identify footpad (FP)-DC subsets. The table inset identifies each subset. (E) Total number of each FP-DC subset, regions 1–4, 3 hours after saline or *E. coli* challenge. N=6. $^{*}p<0.05$ comparing *E. coli* challenged samples to saline controls within each FP-DC subset. Data was analyzed for statistical significance using unpaired Student's *t*-test. Graphical bars represent the mean ±S.D.

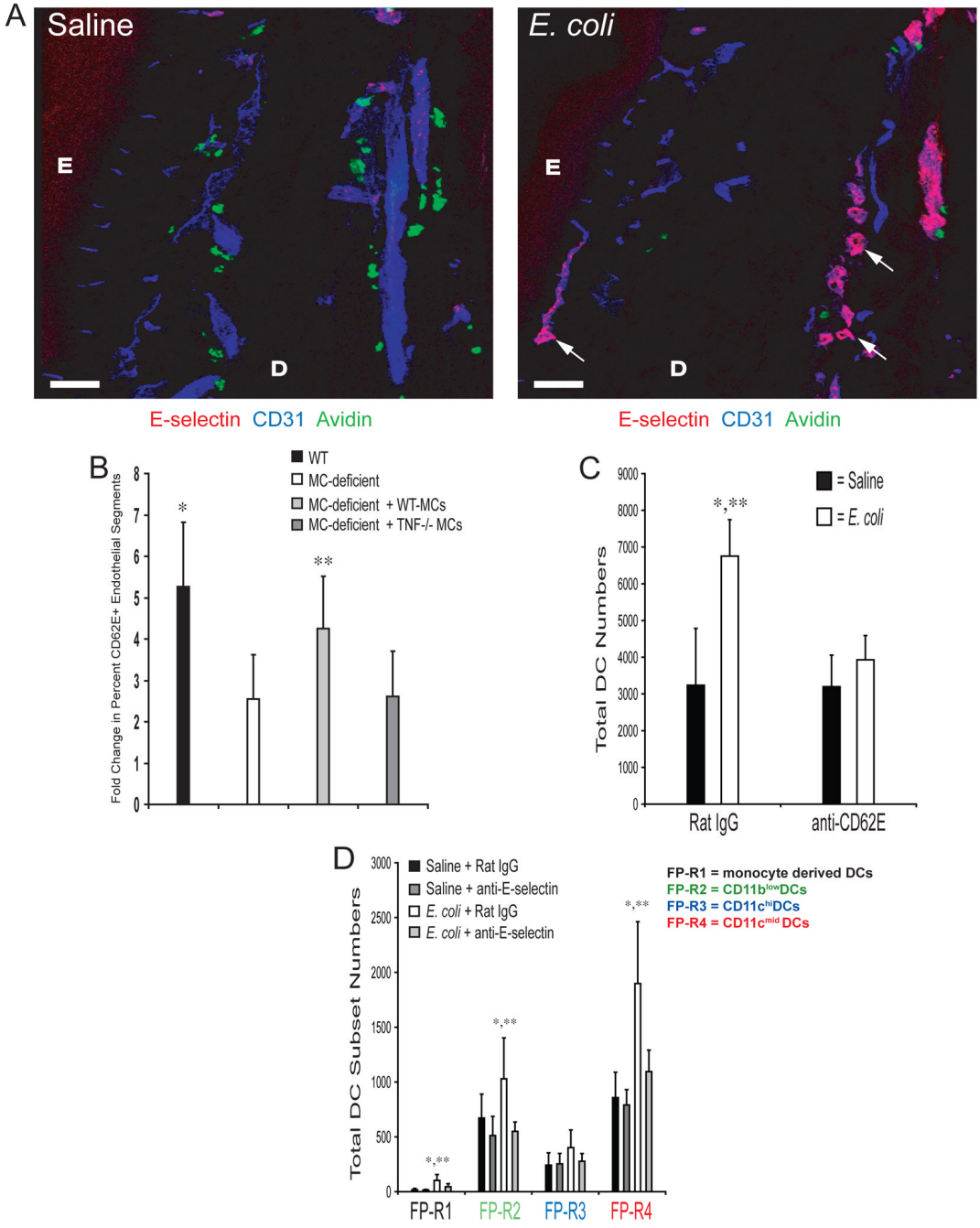

Figure 3. MC-TNF is Required for the Optimal Induction of E-selectin expression after Challenge with *E. coli*

(A) Analysis of WT footpad tissue for E-selectin, CD31 (blood vessel endothelium) and avidin (MCs) by confocal microscopy. E = epidermis, D = dermis. Scale bar = 100μM. Arrows denote $CD62E^+$ endothelial segments. Similar results were obtained in three separate experiments. (B) Enumeration of E-selectin$^+$ blood vessel segments in 700μM × 700μM confocal images derived from 10μM sections of WT, W/W^v, or WT-MC or $TNF^{-/-}$ MC repleted W/W^v footpads, 3 hours after saline or *E. coli* challenge. Data is represented as the *E. coli* induced fold increase in the percent of E-selectin$^+$ blood vessel segments over saline treated controls. N=25–30 fields from three separate experiments. *, **p<0.05 comparing WT or WT-MC

repleted W/W^v samples to W/W^v or $TNF^{-/-}$ MC repleted W/W^v samples, respectively. (C) Total number of $CD11c^+$ DCs in single cell suspensions of footpad 3 hours after challenge with saline or *E. coli*. N=5. $^*p<0.05$ compared to saline controls. $^{**}p<0.05$ comparing *E. coli* challenged samples. (D) Total number of each FP-DC subset, regions 1–4, from mice treated with anti-E-selectin or Rat IgG1, 3 hours after challenge with saline or *E. coli*. N=5. $^*p<0.05$ comparing *E. coli* challenged samples to saline controls within each FP-DC subset, $^{**}p<0.05$ comparing *E. coli* challenged samples from anti-E-selectin to rat IgG1 treated mice within each FP-DC subset. Data in B–D was analyzed for statistical significance with one-way ANOVA and Tukey's post-test. Graphical bars represent the mean ±S.D.

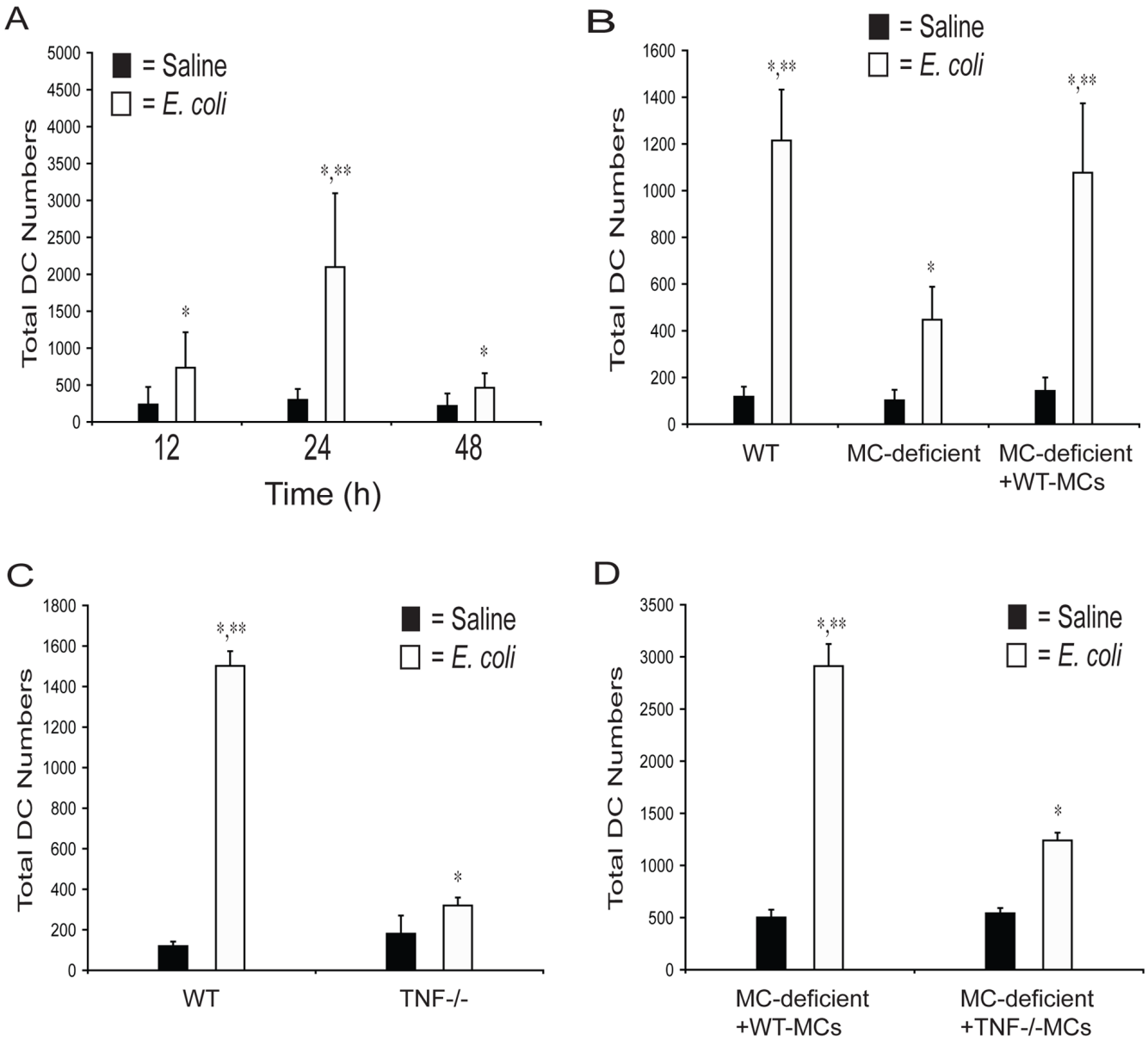

Figure 4. MC-TNF is required to mobilize DCs to DLNs after footpad challenge with *E. coli*

(A) Total number of $CD11c^{+}$/MHC Class II^{+} DCs in single cell suspensions of DLN at 12, 24, or 48 hours after saline or *E. coli* challenge. N≥10 DLNs for each time-point. $^{*}p<0.05$ compared to saline controls. $^{**}p<0.05$ comparing the 24 hour to the 12 and 48 hour *E. coli* challenged samples. (B) Total number of DCs in single cell suspensions of DLNs of WT, W/W^{v}, and WT MC-footpad repleted W/W^{v} mice 24 hours after challenge with saline or *E. coli*. N=6 for WT and W/W^{v} samples. N=4 for MC-repleted W/W^{v} samples. $^{*}p<0.05$ compared to saline controls. $^{**}p<0.05$, comparing *E. coli* challenged MC sufficient samples to the *E. coli* challenged W/W^{v} samples. (C) Total number of DCs in single cell suspensions of DLNs of WT and $TNF^{-/-}$ mice 24 hours after challenge with saline or *E. coli*. N=4 for each sample. $^{*}p<0.001$ compared to saline controls. $^{**}p<0.001$ comparing *E. coli* challenged samples. (D) Total number of DCs in single cell suspensions of DLNs of WT-MC repleted W/W^{v} and $TNF^{-/-}$ MC repleted W/W^{v} mice 24 hours after challenge with saline or *E. coli*. N=4 for each sample. $^{*}p<0.001$ compared to saline controls. $^{**}p<0.001$ comparing *E. coli*

challenged samples. Data in A–D was analyzed for statistical significance with one-way ANOVA and Tukey's post-test. Graphical bars represent the mean ±S.D.

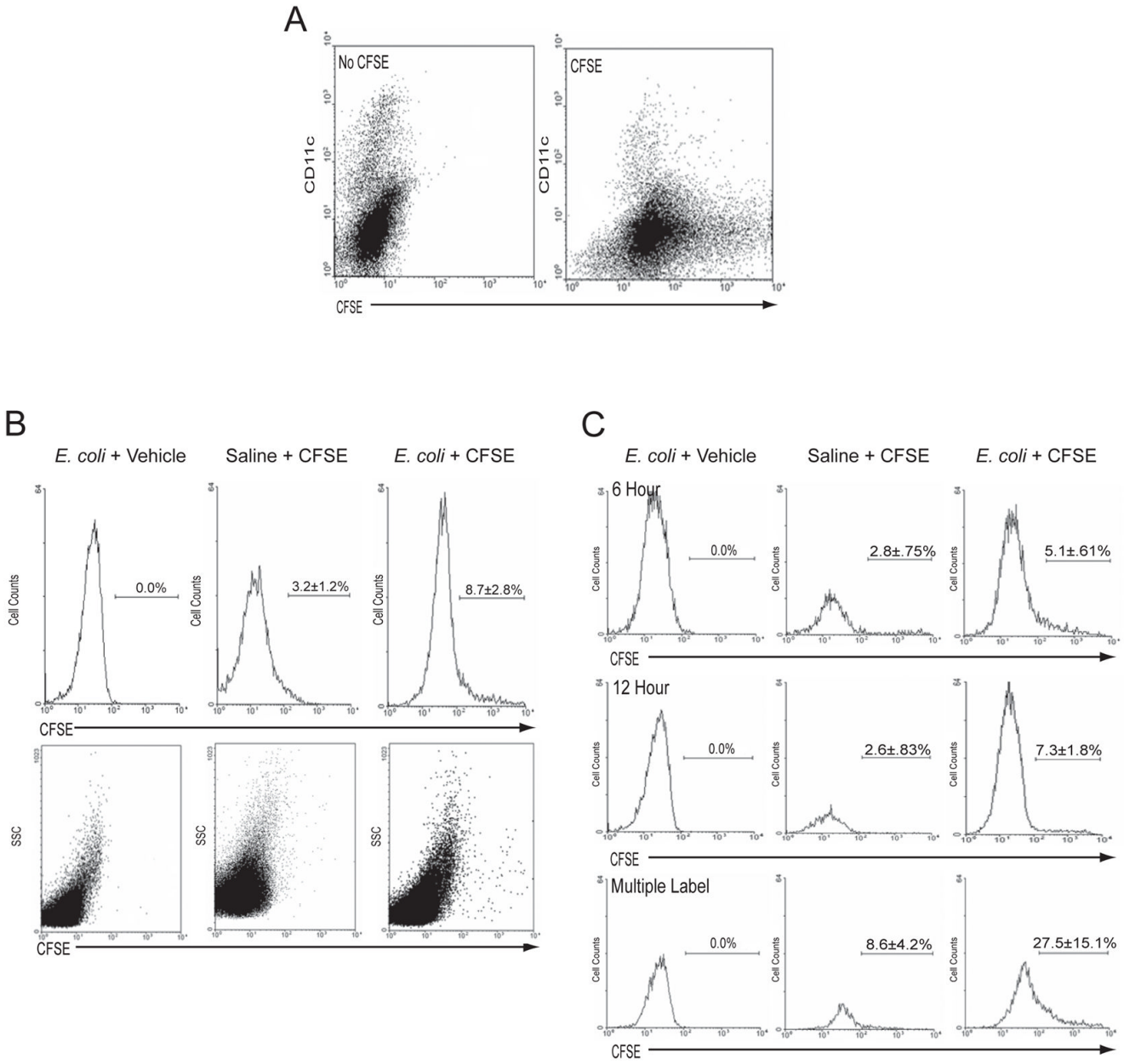

Figure 5. *E. coli* Infection Induces the Continual and Serial Migration of DCs from the Bloodstream through the Footpad prior to their egress to the DLN

(A) CFSE or vehicle was injected into footpads. After 4 hours, single cell footpad suspensions were stained with anti-CD11c and analyzed by flow cytometry. (B) CFSE or vehicle was injected into footpads. After 4 hours, footpads were injected with *E. coli* or saline. After 24 hours, single cell suspensions of DLNs were analyzed by flow cytometry for $CFSE^+$ DCs (identified as $CD11c^+$/MHC Class II^+). The top panel of histograms represents the percentage of $CFSE^+$ DCs in gated DC DLN populations. N=4–6. $p<0.05$ comparing saline to *E. coli* challenged samples. The bottom panels represent the side scatter profile of the entire DLN population of each sample. (C) Footpads were challenged with *E. coli* or saline. At the indicated times, CFSE or vehicle was injected into footpads. 24 hours after saline or *E. coli* challenge, DLN single cell suspensions were stained for DCs (identified as $CD11c^+$/MHC Class II^+) and

analyzed by flow cytometry. Histograms represent the percent of $CFSE^+$ DCs in gated DLN DC populations. Top panels: CFSE or vehicle injected 6 hours after *E. coli* challenge. N=6. $p<0.05$ comparing saline to *E. coli* challenged samples. Middle panels: CFSE or vehicle injected 12 hours after *E. coli* challenge. N=6. $p<0.05$ comparing saline to *E. coli* challenged samples. Bottom panels: CFSE or vehicle was injected 4 hours before, and 6 and 12 hours (multiple label) after *E. coli* or saline challenge. N=6. $p<0.05$ comparing saline to *E. coli* challenged samples. All data was evaluated for statistical significance using unpaired Student's T-test.

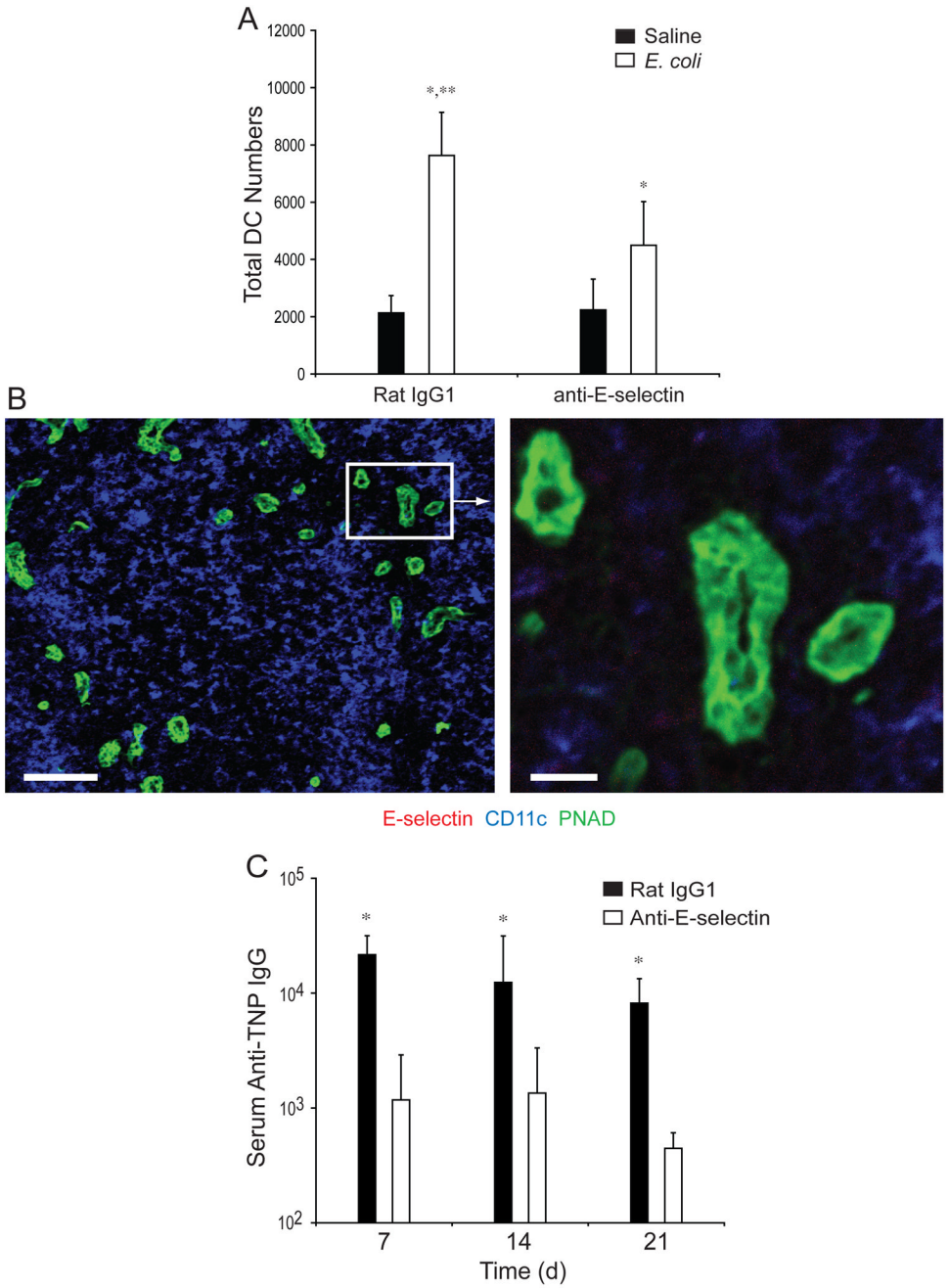

Figure 6. *E. coli* Infection Induces E-selectin dependent increases in DCs in DLNs and humoral responses

(A) Total number of MHC Class $II^+/CD11c^+$ DCs in the DLNs of anti-E-selectin or rat IgG1 treated mice, 24 hours after challenge with saline or *E. coli*. N=3–5. Data was analyzed for statistical significance with one-way ANOVA and Tukey's post-test. $^*p<0.05$ compared to saline controls. $^{**}p=0.01$ comparing *E. coli* challenged samples. (B) Confocal analysis of 10μM sections derived from WT DLNs, 3 hours after *E. coli* challenge. Sections were stained for antiE-selectin, anti-PNAD (high endothelial venules) and anti-CD11c (DCs). Scale bar = 100μM. The boxed inset is represented in the image to the right. Scale bar = 20μM. Similar results were obtained in three separate experiments. (C) GMT of TNP-specific serum IgG in

TNP-*E. coli* challenged mice treated with anti-E-selectin or rat IgG1. N=5 for each group. Significance between saline and *E. coli* challenged samples was evaluated using ANOVA with Tukey's post-test. *p=0.001. Graphical bars represent the mean ±S.D.

Table 1

DC Characterization in the Footpad.

DC Subsets	Markers	Subset	Total Numbers: Saline	Percent Total DC: Saline	Total Numbers: *E. coli*	Percent Total DC: *E. coli*	p Value*
Monocyte derived DCs	$CD11c^{+}CD11b^{hi}GR1^{+}$ (Leon et al., 2007)	FP-R1	26±17	1.2%	90±36	1.9%	0.0007
$CD11b^{lo}$ DCs	$CD11c^{+}CD11b^{lo}GR1^{-}$	FP-R2	831±279	35.5%	1316±194	29%	0.002
$CD11c^{hi}$ DCs	$CD11c^{hi}CD11b^{hi}GR1^{-}$	FP-R3	675±265	30%	897±180	19.5%	0.085
$CD11c^{mid}$ DCs	$CD11c^{mid}CD11b^{hi}GR1^{-}$	FP-R4	779±256	33.3%	2320±585	49.5%	0.00001

*p values comparing total numbers within each DC subset from saline and *E. coli* challenged samples using Student's T-test.